Femtosecond laser direct writing of monocrystalline hexagonal silver prisms

Kevin Vora,[1,a)] SeungYeon Kang,[1,a)] Michael Moebius,[1] and Eric Mazur[1,2]
[1]*School of Engineering and Applied Sciences, Harvard University, 9 Oxford Street, Cambridge, Massachusetts 02138, USA*
[2]*Department of Physics, Harvard University, 9 Oxford Street, Cambridge, Massachusetts 02138, USA*

(Received 13 July 2014; accepted 27 September 2014; published online 10 October 2014)

Bottom-up growth methods and top-down patterning techniques are both used to fabricate metal nanostructures, each with a distinct advantage: One creates crystalline structures and the other offers precise positioning. Here, we present a technique that localizes the growth of metal crystals to the focal volume of a laser beam, combining advantages from both approaches. We report the fabrication of silver nanoprisms—hexagonal nanoscale silver crystals—through irradiation with focused femtosecond laser pulses. The growth of these nanoprisms is due to a nonlinear optical interaction between femtosecond laser pulses and a polyvinylpyrrolidone film doped with silver nitrate. The hexagonal nanoprisms have bases hundreds of nanometers in size and the crystal growth occurs over exposure times of less than 1 ms (8 orders of magnitude faster than traditional chemical techniques). Electron backscatter diffraction analysis shows that the hexagonal nanoprisms are monocrystalline. The fabrication method combines advantages from both wet chemistry and femtosecond laser direct-writing to grow silver crystals in targeted locations. The results presented in this letter offer an approach to directly positioning and growing silver crystals on a substrate, which can be used for plasmonic devices. © *2014 AIP Publishing LLC*.
[http://dx.doi.org/10.1063/1.4897545]

A variety of techniques have been developed to fabricate silver nanostructures.[1–12] Compared to bulk silver, nanocrystals have unique characteristics[13–15] that make them useful for various applications, including catalysis, biomedical sensing, and electronics.[16–22] Wet chemistry is popular for growing high-quality silver crystals in a multitude of shapes, including pyramids, bipyramids, cubes, triangular prisms, hexagonal prisms, and nanowires.[8–11] Wet chemistry, however, lacks patternability. Conversely, femtosecond laser direct-writing methods are used to grow silver in engineered patterns in two and three dimensions.[12,23–28] The resulting structures are composed of aggregates of much smaller silver nanoparticles, often with void or polymer inclusions.[23] We present a method that leads to rapid growth of monocrystalline hexagonal silver nanoprisms through irradiation with focused femtosecond laser pulses. The technique allows us to localize chemical reactions that lead to crystal growth at specific positions on a substrate. The silver structures generated are mostly hexagonal prisms, but some twinned crystals also appear.

To fabricate the nanocrystals, we use a mixture of polyvinylpyrrolidone (PVP), silver nitrate ($AgNO_3$), ethanol, and water. We first prepare a solution by dissolving 0.25 g of PVP in 10 ml of ethanol at room temperature. In a separate vial, we dissolve 0.40 g of $AgNO_3$ in 2.0 ml of deionized water. Once both mixtures are dissolved, we add them together and stir for 25 min. at room temperature. The solution is spin-coated onto a glass slide (1000 rpm for 30 s). Last, the sample is baked in an oven for 25 min. at 110 °C. These steps are done in a room filtered of ultraviolet light to minimize unwanted silver nanoparticle formation. The resulting sample consists of a micrometer-thick polymer film doped with silver ions on a glass substrate.

We use a Ti:sapphire laser centered at 795 nm with an 11-MHz repetition rate and 300-fs pulse duration for the irradiation process. A description of the laser fabrication setup can be found in Ref. 23. A tightly focused laser beam is scanned onto the sample to produce a periodic array of irradiation sites. The laser exposure is limited to individual voxels inside the PVP film, at the glass-polymer interface. The laser focal diameter is approximately 1 μm (full-width half-max) using a 0.8 NA microscope objective.

In-situ optical imaging shows that silver growth occurs at nearly 100% of the irradiation spots. However, after irradiation, the polymer film must be dissolved with water or ethanol for sample analysis, leaving behind only those silver nanostructures that strongly adhere to the glass substrate. Scanning electron microscopy (SEM) image analysis reveals the yield of silver adhering to irradiation sites after polymer removal is approximately 5%. This low yield is due to insufficient adhesion between crystals and the substrate. We expect to achieve higher yields with additional pre-treatment steps that increase adhesion. Within the adhered structures, 45% are crystals with hexagonal shaped bases (6 facets with 120° internal angles), 21% are partially ablated or cracked hexagonal crystals, 15% are crystals with hexagonal-like bases (which have small deformations, or greater than 6 facets, with additional facets positioned with 120° or −120° internal angles), and 12% are twinned crystals.

Several experimental parameters can be tuned or can fluctuate during the fabrication process, including pulse energy, exposure time, focus position, laser stability, as well as local variations in the polymer film or substrate. These conditions can affect both shape and size of silver structures grown through femtosecond laser irradiation. However,

[a)]Kevin Vora and SeungYeon Kang have made equal contributions to the present work.

despite variations, the fabrication process primarily produces prisms with bases having 120° or −120° internal angles, as opposed to potential alternate morphologies, such as nanoparticle aggregates, triangular prisms, cubes, or disks. More specifically, the yield from the method is dominated by large prisms with hexagonal shapes.

The crystals in Figure 1 are representative of the hexagonal prisms grown through the fabrication process. Figure 1(a) shows a high magnification SEM image of a 900-nm crystal grown with a total exposure time of 100 μs and 4.1 nJ per pulse; Figure 1(b) shows an SEM image of a 500-nm crystal grown with an exposure of 800 μs and 1.5 nJ per pulse. Fabricated crystals vary in size between 400 nm and 1 μm. The laser exposure pattern can be observed in Figure 2 (the dark spots on the substrate indicate laser exposure sites where silver structures were detached during the polymer removal step). Figure 2(a) shows two hexagonal crystals grown in neighboring positions with different sized bases, with a high magnification image in Figure 2(b). Figure 2(c) shows six crystals grown in proximity to each other, each with varying deformations. Two of the crystals are shown with higher magnification in Figure 2(d): The left crystal is twinned and the right crystal has greater than 6 facets.

Figure 3 shows an SEM image of a hexagonal crystal grown at an exposure of 800 μs and its corresponding energy dispersion x-ray spectroscopy (EDS) elemental maps. The EDS elemental maps show that the nanocrystal is composed of silver. We further characterized the crystals through electron backscatter diffraction (EBSD) measurements, which provide information on the orientation and crystal structure of a material. Figure 4 shows EBSD measurements indicating a single-crystal FCC lattice structure in the hexagonal crystal, consistent with monocrystalline silver. Figure 4(b) shows uniform grain orientation and phase distribution with no grain boundary, and Figure 4(d) shows the crystallographic orientation of the fabricated silver nanocrystal. The (100) pole plot in Figure 4(c) represents a stereographic projection of the crystallographic directions present in the grains that make up the material. All individual point orientation measurements from the sample are shown together as three closely packed clusters of points on the pole figure representing the (100), (010), and (001) planes of the sample. These results indicate that probed portions of the silver structure are single-crystal; the hexagonal silver structures are monocrystalline, unlike silver grown through previously reported femtosecond laser techniques.[12,23–29] From the EDS and EBSD analyses, we conclude that under appropriate conditions, the femtosecond-laser direct metal writing leads to single-crystal particle growth.

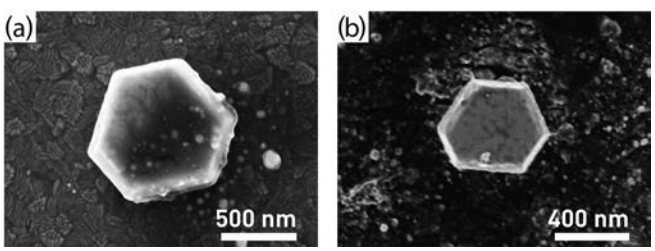

FIG. 1. SEM images of (a) 900-nm and (b) 500-nm crystals grown by irradiation with a 795-nm femtosecond laser with a total exposure time of (a) 100 μs and 4.1 nJ per pulse and (b) 800 μs and 1.5 nJ per pulse.

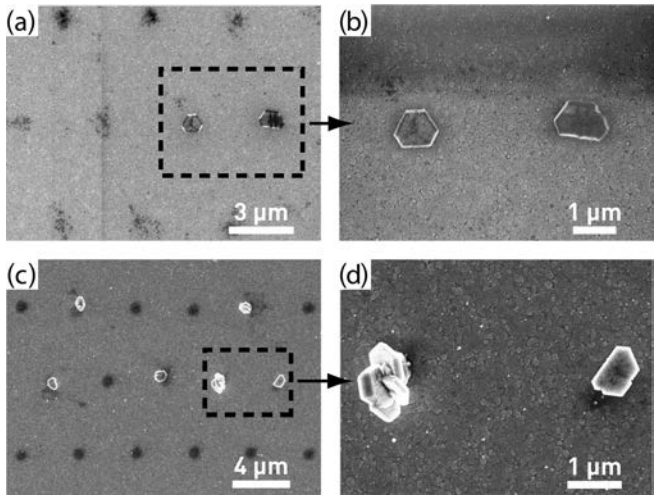

FIG. 2. Sample preparation for SEM imaging removes all structures not strongly adhered to the substrate. These SEM images show silver crystals that remain attached to the glass. (a) Image showing two silver crystals grown in neighboring laser irradiation spots. (b) A close-up view reveals both crystals are hexagonally shaped and have different sized widths. (c) Image showing six crystals grown in proximity to each other. (d) A close-up view reveals two silver structures that are not single crystal hexagonal prisms. The left structure is a twinned crystal. The right structure is a crystal where the internal angles are ±120°.

Previous femtosecond laser fabrication work by Baldacchini *et al.* and Maruo *et al.* using similar chemical preparation methods yielded aggregates of small silver nanoparticles; they did not observe any silver crystal growth.[25,26] Whilst their sample preparation methods were similar, they used significantly lower pulse energies during laser exposure, ranging between 0.013 and 0.46 nJ per pulse.[25,26] Their peak intensities were approximately one to two orders of magnitude lower than the present work, suggesting a minimum energy density threshold to obtain crystal growth. Chemistry also plays a crucial role in the growth process. In

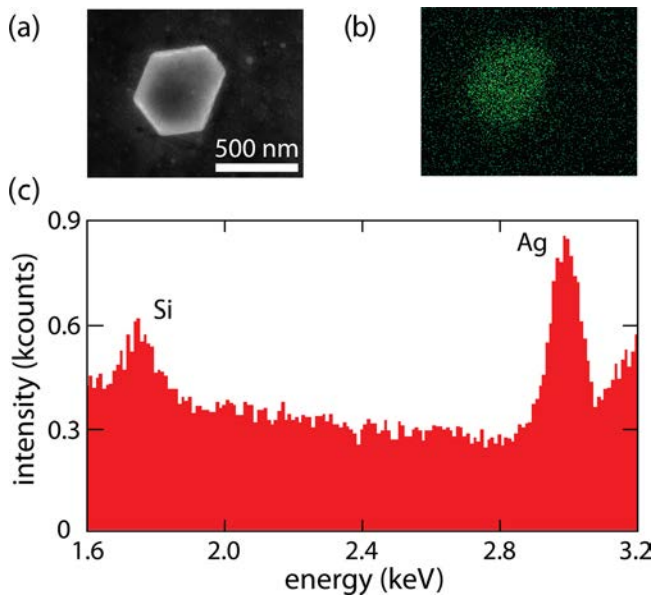

FIG. 3. (a) SEM image of a 500-nm crystal, (b) corresponding silver EDS map, and (c) EDS spectrum. The map shows a silver signal concentrated at the location of the nanocrystal, demonstrating high silver content. The silicon signal originates from the sample substrate.

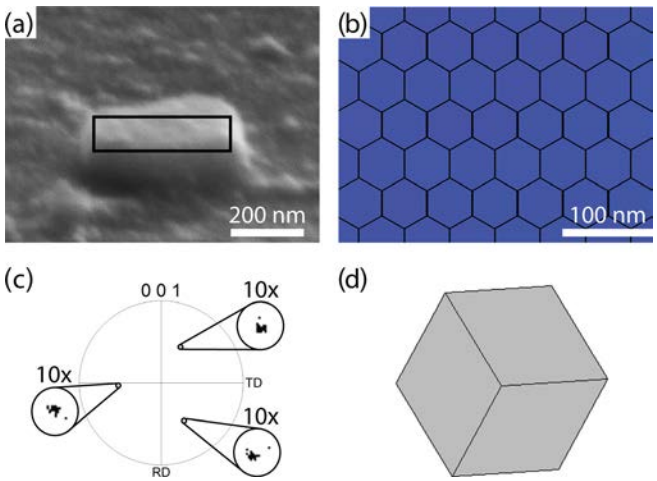

FIG. 4. SEM image of a silver 400-nm nanocrystal and corresponding EBSD data showing single crystal structure. (a) SEM image taken from a 70° angle; outline shows the area mapped with EBSD. (b) The honeycomb contour in the EBSD map outlines the individually probed pixels; the color uniformity is indicative of single crystal orientation. (c) The (001) pole figure further highlights single crystal orientation; the insets show a 10× close-up. RD refers to sample rolling direction and TD refers to transverse direction. The silver crystal orientation is shown in (d), where the substrate is in the plane of the page.

previously reported work, we used water rather than a mixture of water and ethanol to dissolve the solutes.[23,29] This method only produced nanoparticle aggregates, and we did not observe any monocrystalline silver structures in the absence of ethanol.[23,29] The present report highlights the need for carefully selected laser parameter and material combinations to obtain silver crystal growth during femtosecond laser fabrication.

During growth using wet chemistry, the shape and size of silver crystals can be tuned by varying the chemical composition and reaction time.[7,9,10] The strong affinity of N and O atoms in the amide groups of PVP to surfaces of transition-metal clusters restrains the growth of these clusters. Because PVP interacts preferentially with {100} planes in silver crystals, it leads to faster growth in specific crystal directions.[9,10] However, the size and shape of the nanocrystals produced with the laser technique described in this letter are rarely observed using wet chemistry even when the same chemical reagent mixture is used.[11,22] Furthermore, traditional wet chemistry is relatively slow; at a typical refluxing temperature of 120 °C to 160 °C, it takes between 0.5 and 30 h to grow silver crystals between 80 nm and 280 nm in size.[8–11] We use exposure times that are over 8 orders of magnitude shorter, and yet obtain much larger crystals. Such ultrafast growth of silver crystals has not been previously reported. This suggests that non-equilibrium dynamics arising from the femtosecond excitation[30] play a role in the growth of the hexagonal nanoprisms.

As described in the supplementary material,[35] irradiation with femtosecond laser pulses leads to plasmon resonances during crystal growth. Studies on the synthesis of silver nanostructures in liquid solution have shown that plasmon resonances can play a role in directing crystal growth through three primary types of surface plasmon-mediated photophysical effects: local heating of nanoparticles and surrounding environments, high electromagnetic fields and photon fluxes for molecules near nanoparticle surfaces, and charge transfer reactions between nanoparticles and nearby molecules through energetic electron-hole pair generation.[31] A detailed understanding of the contributions of each effect remains elusive;[31,32] however, we expect a combination of these factors to enhance chemical reaction rates near nanoparticles during femtosecond fabrication. Furthermore, laser irradiation may enhance the coalescence of nanoparticles by decreasing the magnitude of silver nanoparticle zeta potential[32] and inducing PVP ligand dissociation through high electromagnetic fields,[31] further increasing the growth rate.

Plasmon-mediated growth of silver crystals strongly depends on many factors, including metal source, stabilizing agent, reducing agent, solvent, and optical irradiation parameters.[31–34] The present work is further complicated from previously studied systems by the use of ultrashort pulses with very high peak intensity (on the order of terawatts per square centimeter), and a cured thin film growth medium that limits particle mobility. There are many unanswered questions about the details of the crystal growth mechanism during femtosecond laser fabrication. Additional experimental studies are required to elucidate the growth process and understand the interplay between photochemical and plasmon-enhanced reactions.

In conclusion, the femtosecond laser method we describe localizes chemical reactions that lead to nanoscale silver crystal growth at specific positions on a substrate. We grow silver structures with a yield dominated by hexagonal prisms. The use of femtosecond laser irradiation dramatically increases the growth speed and size of nanocrystals compared to traditional techniques; we obtain hexagonal shapes that are hundreds of nanometers in size with sub-millisecond laser exposure. By fine-tuning the laser parameters, chemical reagents, and silver adhesion, the technique outlined in this letter may be modified to finely control the shape and size of silver crystals, and increase yield. This could present a significant advancement for the fabricating of plasmonic devices.

The research described in this paper was supported by the Air Force Office of Scientific Research under Grant Nos. FA9550-09-1-0546 and FA9550-10-1-0402. The authors acknowledge the use of facilities in the Center for Nanoscale Systems, which is supported by the National Science Foundations National Nanotechnology Infrastructure Network, and the assistance provided by Dave Lange with EBSD measurements. Yu-Ting Lin and Orad Reshef provided feedback on the manuscript throughout its development.

[1]P. D. Nallathamby, K. J. Lee, and X. H. N. Xu, ACS Nano **2**, 1371 (2008).
[2]F. Mafune, J. Kohno, Y. Takeda, T. Kondow, and H. Sawabe, J. Phys. Chem. B **104**, 8333 (2000).
[3]A. Pal, S. Shah, and S. Devi, Mater. Chem. Phys. **114**, 530 (2009).
[4]C. M. Gonzalez, Y. Liu, and J. C. Scaiano, J. Phys. Chem. C **113**, 11861 (2009).
[5]C. M. Soukoulis and M. Wegener, Nat. Photonics **5**, 523 (2011).
[6]R. A. Salkar, P. Jeevanandam, S. T. Aruna, Y. Koltypin, and A. Gedanken, J. Mater. Chem. **9**, 1333 (1999).
[7]M. Starowicz, B. Stypula, and J. Banas, Electrochem. Commun. **8**, 227 (2006).
[8]J. H. Zhang, H. Y. Liu, P. Zhan, Z. L. Wang, and N. B. Ming, Adv. Funct. Mater. **17**, 1558 (2007).

[9]Y. G. Sun and Y. N. Xia, Science **298**, 2176 (2002).
[10]B. Wiley, Y. G. Sun, B. Mayers, and Y. N. Xia, Chem. Eur. J. **11**, 454 (2005).
[11]J. S. Kim, J. Ind. Eng. Chem. **13**, 566 (2007).
[12]M. M. Mariscal, J. J. Velazquez-Salazar, and M. J. Yacaman, Crystengcomm **14**, 544 (2012).
[13]A. Thiaville and J. Miltat, Science **284**, 1939 (1999).
[14]T. Bein and G. D. Stucky, Chem. Mater. **8**, 1569 (1996).
[15]G. A. Ozin, Adv. Mater. **4**, 612 (1992).
[16]Z. H. Huang, X. L. Jiang, D. W. Guo, and N. Gu, J. Nanosci. Nanotechnol. **11**, 9395 (2011).
[17]D. T. Schoen, A. P. Schoen, L. B. Hu, H. S. Kim, S. C. Heilshorn, and Y. Cui, Nano Lett. **10**, 3628 (2010).
[18]D. P. Chen, X. L. Qiao, X. L. Qiu, and J. G. Chen, J. Mater. Sci. **44**, 1076 (2009).
[19]K. J. Lee, B. H. Jun, T. H. Kim, and J. Joung, Nanotechnology **17**, 2424 (2006).
[20]Z. J. Jiang, C. Y. Liu, and L. W. Sun, J. Phys. Chem. B **109**, 1730 (2005).
[21]P. Jain and T. Pradeep, Biotechnol. Bioeng. **90**, 59 (2005).
[22]P. Alivisatos, Nat. Biotechnol. **22**, 47 (2004).
[23]K. Vora, S. Kang, S. Shukla, and E. Mazur, Appl. Phys. Lett. **100**, 063120 (2012).
[24]Y.-Y. Cao, N. Takeyasu, T. Tanaka, X.-M. Duan, and S. Kawata, Small **5**, 1144 (2009).
[25]T. Baldacchini, A.-C. Pons, J. Pons, C. LaFratta, J. Fourkas, Y. Sun, and M. Naughton, Opt. Express **13**, 1275 (2005).
[26]S. Maruo and T. Saeki, Opt. Express **16**, 1174 (2008).
[27]T. Tanaka, A. Ishikawa, and S. Kawata, Appl. Phys. Lett. **88**, 081107 (2006).
[28]A. Ishikawa, T. Tanaka, and S. Kawata, Appl. Phys. Lett. **89**, 113102 (2006).
[29]K. Vora, S. Kang, and E. Mazur, J. Vis. Exp. **69**, e4399 (2012).
[30]S. K. Sundaram and E. Mazur, Nat. Mater. **1**, 217 (2002).
[31]M. R. Langille, M. L. Personick, and C. A. Mirkin, Angew. Chem. Int. Ed. **52**, 13910 (2013).
[32]T. Tsuji, T. Mizuki, S. Ozono, and M. Tsuji, J. Photochem. Photobiol. A **206**, 134 (2009).
[33]X. Wu, P. L. Redmond, H. Liu, Y. Chen, M. Steigerwald, and L. Brus, J. Am. Chem. Soc. **130**, 9500 (2008).
[34]X. Zheng, W. Xu, C. Corredor, S. Xu, J. An, B. Zhao, and J. R. Lombardi, J. Phys. Chem. C **111**, 14962 (2007).
[35]See supplementary material at http://dx.doi.org/10.1063/1.4897545 for methods and discussion on plasmon resonances.